

# Shear tests evaluation and numerical modelling of shear behaviour of reinforced concrete beams

András Draskóczy

Received 2009-03-19

## Abstract

A series of 24 reinforced concrete beams – amongst them six prestressed – were tested in the laboratory of the Department of Mechanics, Materials and Structures, TUB in 2005. The principal aim of the research program was to develop the variable strut inclination method used for shear design of reinforced concrete beams by Eurocode 2. Based on numerical evaluation of a substitutive vaulted lattice model with compressed-sheared top chord and some experiences of the test results, the author proposes to increase the fraction of the shear force attributed to the concrete in simple supported reinforced concrete beams loaded by a uniformly distributed load. Attention is drawn to the importance of adequate anchorage of the horizontal component of the diagonal concrete compression force at the supports.

## Keywords

reinforced concrete · shear · variable strut inclination · testing · D-region · vaulted lattice model

## Acknowledgement

I am very much obliged to Mr László Polgár technical director of the ASA Building Construction Company for his considerable help in joining the research project and supplying the test beams from their prefabrication plant in Hódmezővásárhely, 180 km from Budapest. Without the financial support of the Research Development Competition and Research Application Bureau of the Hungarian Ministry of Education testing of beams could not have been realized. Many thanks to Ottó Sebestyén who carried out an enormous amount of work with the preparation of the test beams. I would also like to express my acknowledgement to my colleagues University Professor László Kollár, member of the Hungarian Academy of Sciences, Professor Emeritus Endre Dulácska, Associate Professor István Sajtos, Assistant Professor István Hamza and Electrical Engineer Miklós Kálló for their numerous advice.

## András Draskóczy

Department of Mechanics, Materials and Structures, BME, H-1111 Budapest  
Műegyetem rkp. 3. K 242., Hungary  
e-mail: drasko.sil@silver.szt.bme.hu

## 1 Introduction

Within the framework of a three year research project financed by the Hungarian Ministry of Education and in cooperation with the ASA Building Construction Company, a series of 24 reinforced concrete beams – amongst them six prestressed – were tested in the laboratory of the Department of Mechanics, Materials and Structures, TUB in 2005. The principal aim of the investigation was formulated by the author [1] by emphasizing the need for more detailed information about preconditions of the application of the variable strut inclination method for shear design of reinforced concrete beams outlined by Eurocode 2 (EC2) [2]. Improper anchorage of the tensile reinforcement at extreme supports may cause premature failure if little strut inclination angle is presumed by the designer at the shear design of the beam. 4 m and 7.6 m span beams were tested, subjected to a uniformly distributed load. The principal variable parameters investigated were stirrup spacing and anchorage conditions. Results of the test evaluation and proposals for the development of the variable strut inclination method will be treated by the author.

## 2 Test program

### 2.1 Characteristics of the test beams

Six series of 4 beams each were tested. The T-shaped cross section had a 500 mm depth, a 500 mm flange width and a 160 mm web width. The strength grade of the concrete was about C30/37, compression strength was tested on cubes before testing of the beam. Steel B60.50, Fp100-1770 prestressing strands and BHB55.50 used for stirrups were applied. Beam type A (12 pieces) had 4.25 m total length and were elastically supported along 250 mm at both ends. The support length of beam type B (8 pieces) was 100 mm and had the same effective length of 4.00 m as beam type A. The  $l_{\text{eff}}/d$  rate of these beams was about 10. There were four variants (denoted by K1 to K4) of link spacing investigated: 50, 100, 200 and 300 mm (see Fig. 1).

Tension reinforcement was  $4 \times 3\text{Ø}16$  bars. By one 4 beams-series of B-type beams  $9\text{Ø}16$  bars were substituted by  $2 \times 3\text{Fp}100$  prestressing strands. Three variants of the longitudinal nonprestressed reinforcement were tested: full length bars,

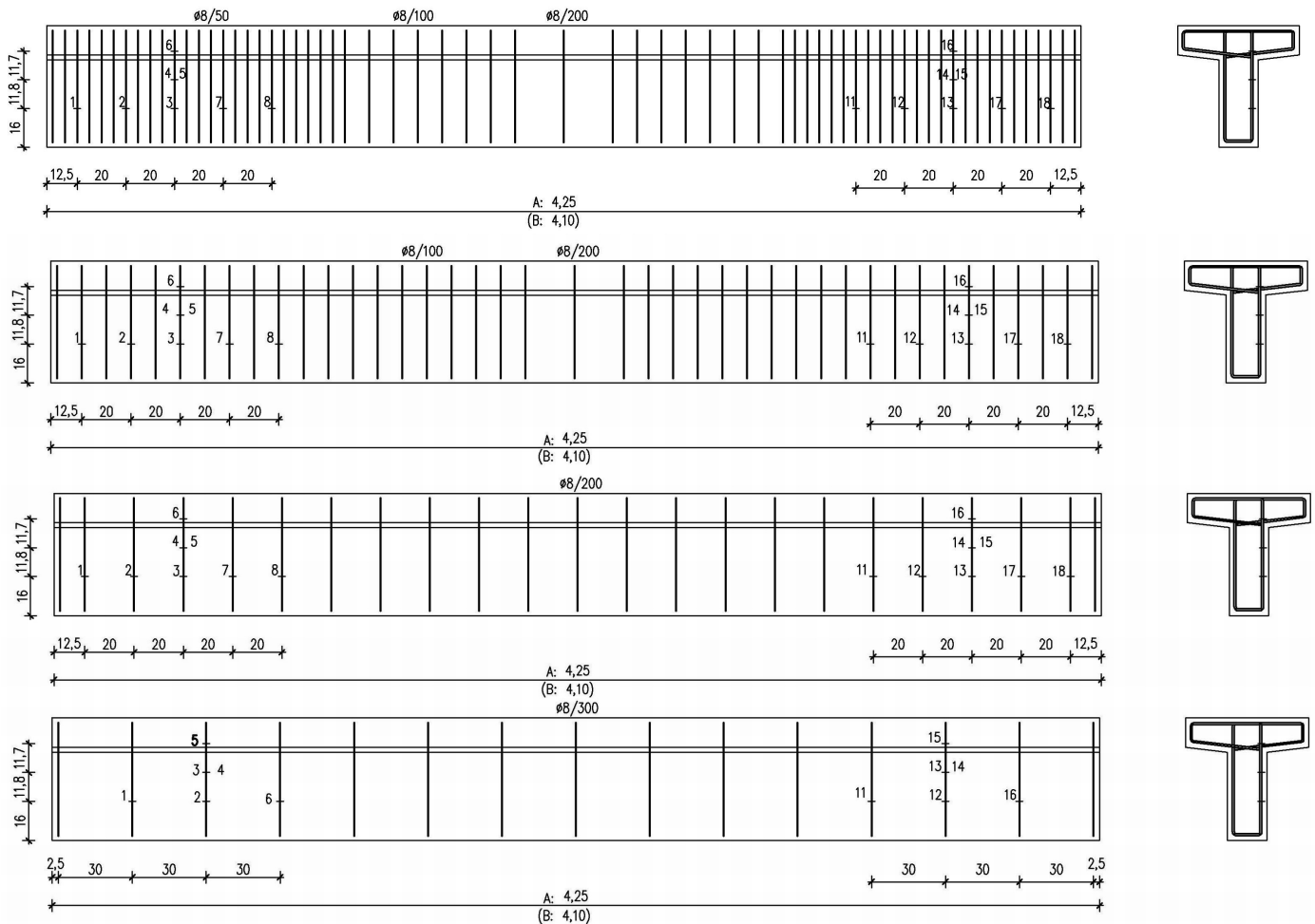


Fig. 1. Link spacing of 4 m span beams

2×3 bars cut corresponding to enveloping the moment diagram and this latter combined with two internal bars hooked at the end of the beam. Four 7.6 m span beams (type C) were also tested with  $l_{eff}/d = 20$ , two of them prestressed. Constructional rules of EC2 were respected by detailing the reinforcement.

## 2.2 The load application method

Uniformly distributed load was applied through water pressure created in a fibre reinforced PVC sack. The width of the sack had to be increased to produce the maximum ultimate load intensity of about 320 kN/m by making use of water-system pressure of 4.2 at. Steel frame and timber boards were used as pressure transmission devices between water sack, beam and steel frame of the loading equipment respectively. Load intensity was controlled through an 8 channel amplifier, by measuring the support reaction forces. Load was applied in steps of about 1/10 of the ultimate loading. Mean duration of one test was four hours.

## 2.3 Measurements

Concrete deformations were measured using manual deformeters on 2×3 8- point rosettes of 60 mm diameter. At midspan, contraction of concrete near to the extreme compression

fibre was also registered. Signals of strain gages stuck to 2×3 links near to the supports and to the centre bottom Ø16 bar at midspan and along its anchorage length were recorded by a computer controlled scanner system. Retraction of the tension reinforcement at the extremities and the deflection at midspan were also electronically controlled by the 8 channel amplifier. End rotations and opening of some major cracks were measured manually. Crack patterns were drawn by using different colour pens at higher load intensities.

## 3 Control calculations for different compression strut inclinations

### 3.1 Control calculations

Statistical evaluation of the concrete compression strength was carried out based on rupture test results measured on 5 pieces of 150 mm cubes. Characteristic and design values of resistance forces corresponding to four different failure modes were computed: flexural failure ( $M_R$ ), compression failure of concrete due to shear ( $V_{R,max}$ ), tension failure of the shear reinforcement ( $V_{R,s}$ ), slip of tension reinforcement at beam end ( $F_{R,s}$ ). The load intensity at failure is in three cases of these four failure modes depending on the compression strut inclination angle  $\theta$ . Characteristic and design load capacities cor-

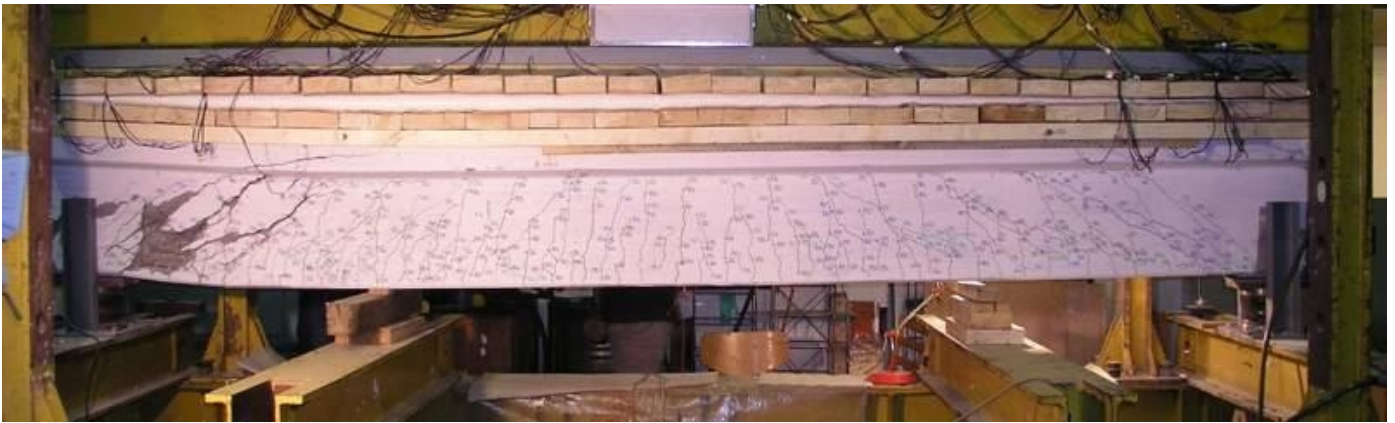


Fig. 2. Load application method and rupture of beam AN1K4

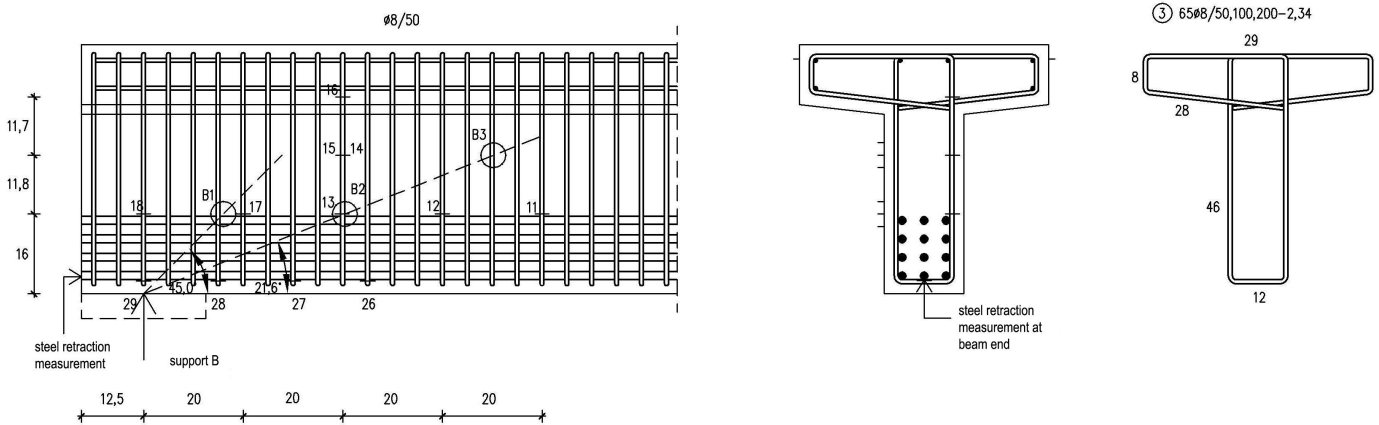


Fig. 3. Measurements at beam end type AN1K1

responding to the different failure modes were determined for each test beam and for compression strut inclination angles  $\theta$  varying between  $21.6^\circ$  and  $45^\circ$  according to formulae and expressions given in [2]. For prestressed beams prestress loss due to elastic deformation, relaxation, shrinkage and creep were determined by respecting the technology and type of products – 7-wire strands, cement class R – used, the concrete strength, ambient conditions and the duration of time that elapsed between fabrication and testing.

### 3.2 Strut inclination angle and maximum load capacity

The calculated design load capacity corresponding to the mode of failure reached first was determined for different compression strut inclination angles  $\theta$  between  $21.6^\circ$  and  $45^\circ$ . From among these values the maximum design load capacity and the corresponding compression strut angle was considered and compared with the rupture load intensity and mode of failure at test. Results for beams type A can be seen in Table 1. The definition of the beam code letters are: A: 250 mm support length, N1 to N3: three variants of tension reinforcement of normal, non-prestressed beams, as given in 2.1, K1 to K4: four variants of stirrups as given in 2.1.

Tab. 1. Capacities and failure modes of test beams

Beam code	$p_{Rdmax}$ (kN/m)	$\theta$ ( $^\circ$ )	reason of reaching $p_{Rdmax}$	$p_u/p_{Rdmax}$	reason of failure
AN1K1	184.0	45	$M_{Rd}$	1.73	$M_{Ru}$
AN1K2	166.7	35	$V_{Rds}$	1.79	$M_{Ru}$
AN1K3	125.2	25	$V_{Rds}$	2.10	$F_{Rsu}$
AN1K4	98.3	22	$V_{Rds}$	2.73	$F_{Rsu}$
AN2K1	186.2	45	$M_{Rd}$	1.54	$M_{Ru}$
AN2K2	179.7	30	$F_{Rds}$	1.72	$M_{Ru}$
AN2K3	132.3	22	$F_{Rds}$	1.86	$F_{Rsu}$
AN2K4	98.3	22	$V_{Rds}$	2.17	$F_{Rsu}$
AN3K1	181.9	45	$M_{Rd}$	1.65	$M_{Ru}$
AN3K2	166.7	35	$V_{Rds}$	1.46	$F_{Rsu}$
AN3K3	132.3	22	$F_{Rds}$	1.92	$F_{Rsu}$
AN3K4	98.3	22	$V_{Rds}$	1.97	$F_{Rsu}$

## 4 Evaluation of test results

### 4.1 Ultimate loads and failure modes

17 of the 24 test beams failed for shear. Calculated and real failure modes were in some cases different. The characteristic difference was that according to measured strain gauge data reaching of the maximum capacity load was followed by sudden bound failure of the tension reinforcement at beam extremity.

Although excessive opening of shear cracks seemed to testify yield of the stirrups, strain gauge signals did not always support this and rupture of the stirrups did not occur in any cases.

#### 4.2 Rates of measured and calculated load capacities

Rates of rupture load per calculated design load capacity are given in Table 1 above for beams type A. It can be observed that the highest rates were obtained for cases when the calculated design load capacity corresponded to tension failure of links due to shear. This demonstrates that design resistance expressed by  $V_{Rds}$  determined according to [2] is too conservative. The regions of beams near supports are subjected to the highest shear forces, but due to the diagonal introduction of the concentrated support reaction force and – at extreme supports – the introduction of the equilibrating internal tension force component in the bottom reinforcement results in a local situation which should be handled in a way somewhat different from the parallel chord lattice model of Mörsh. In D-regions near beam extremities the diagonal compression acting in the concrete contributes to the equilibration of shear forces. This is the main reason why the shear capacity  $V_{Rds}$  is underestimated. In the very same cases the real reason for failure is the bond failure along the anchorage length of the tensile reinforcement, a problem which should be handled with more care, and which is in direct relation with the compression strut inclination angle. The proposed model for D-regions at beam extremities is treated in Section 5.

#### 4.3 Load levels corresponding to serviceability limit states

Load levels corresponding to reaching serviceability limit state situations of crack opening and deflection were also registered, but their presentation is outside of the scope of this paper.

### 5 Vaulted lattice model with compressed-sheared top chord of reinforced concrete beams

#### 5.1 The vaulted lattice model

In the following, simply supported reinforced concrete beams will be investigated with a constant concrete section, loaded with a uniformly distributed load and supplied with vertical stirrups. Supporting the tied arch model-creation idea mentioned by Walther (1956), Polónyi (1996), Schlaich (1998), the author will propose certain refinements on the parallel chord lattice model of Mörsh. The essence of the proposal is to consider the line of action of the resultant of top chord compression stresses of reinforced concrete beams – the so called compression line – to be the compression chord axis of the lattice model of Mörsh. This compression line is arched and intersects the horizontal bottom chord axis – the axis of the tension reinforcement – above the theoretical support point under an angle  $\theta_A$ .

The vaulted compression line can approximately be determined. When applying the vaulted lattice model for shear design, it is to be emphasized that the vertical component of the concrete compression force acting along the compression line can be considered as part of the shear capacity, which, just at the maximum

of the actual shear force is significantly reducing the shear force fraction to be equilibrated by the shear reinforcement.

$$V_{Rd,\gamma}(x) = N_{cV}(x) = N_{cH}(x) \tan \gamma(x), \quad (1)$$

where  $V_{Rd,\gamma}$  is part of the design shear capacity due to the vertical component of the concrete compression force,  $N_{cV}$  and  $N_{cH}$  are components of the force developing in the concrete compression chord,  $\gamma(x)$  is the direction angle of the compression line at distance  $x$ .

The shear capacity fraction attributed to the concrete should be limited from above. We accept – and take into consideration in the numerical examples below – that

$$V_{Rd,\gamma} \leq V_{Rd,max}, \quad (2)$$

is the design value of the shear capacity fraction attributed to the concrete and should not be greater than the design value of the greatest actual shear force, limited by fracture of the inclined concrete compression struts according to EC2.

The proposed modified lattice model will really be regarded as one with variable strut inclination angle along the beam axis. The strut inclination angle at the point of intersection of the interior support face and of the bottom plane of the member will be assumed to be equal to  $\theta$  as given in EC2, where it is regarded constant. Although the direction coordinate  $x$  is measured from the left support  $A$  parallel to the beam axis, but variation of the strut inclination angle  $\theta(x)$  will be interpreted along the compression line, because compression strut forces branch off from the compression line. The strut inclination angle  $\theta(x_1)=\theta$ , because the strut with inclination angle  $\theta$  branches off from the point  $(x_1, z(x_1))$  of the compression line, and intersects the bottom plane of the member just at the interior edge of the support (see Fig. 4) which means that

$$\cot \theta(x_1) = \cot \theta = \frac{x_1 - a_i}{z(x_1) + d_1} \quad (3)$$

The coordinate  $x_1$  is determined by numerical approximation when determining the compression line. Along the left half beam axis two sections as given below will be distinguished.

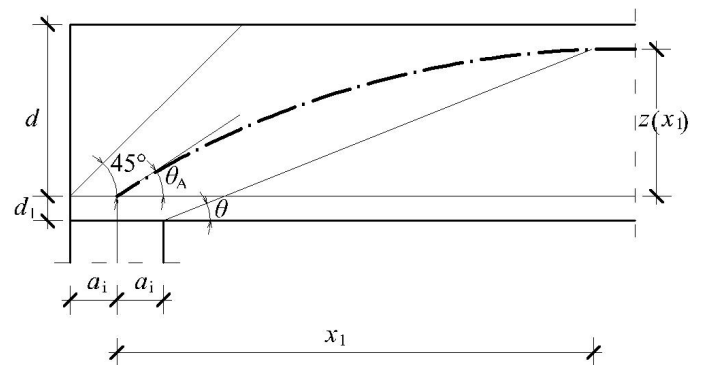


Fig. 4. Modelling of the D-region

The section  $0 \leq x \leq x_1$  can be characterized by fan-wise spreading compression forces in the concrete. The top corner of

the beam end does not play a significant role in transmitting the support reaction force, so that it can even be cut down by a 45° diagonal plane above the bottom reinforcement (see Fig. 5). As an approximation, the strut inclination  $\theta_A$  at  $x=0$  can be considered equal to the arithmetic mean value of 45° and  $\theta$ :

$$\theta_A = \frac{45^\circ + \theta}{2} \quad (4)$$

Along section  $0 \leq x \leq x_1$  the strut inclination angle will approximately be regarded linearly variable:

$$\theta(0 \leq x \leq x_1) = \theta_A - \frac{x}{x_1}(\theta_A - \theta) \quad (5)$$

The section  $x_1 \leq x \leq 0.5l$  can be characterized by variable strut inclination angles also because of cracks getting steeper in direction of the centre of span. This variation will also be approximated by linear function between  $\theta$  and 45°:

$$\theta(x_1 \leq x \leq 0.5l) = \theta + \frac{x - x_1}{0.5l - x_1}(45^\circ - \theta) \quad (6)$$

On Fig. 5 the variation of  $\theta(x)$  is shown along the left half beam axis using data of one of the numerical examples. The variation expresses, that the shear force fraction that can be transmitted by cracking friction is decreasing in the direction of the interior of the span.

## 5.2 Determination of the compression line

Points of the compression chord axis of the vaulted lattice model indicated on Fig. 5 are lying on a curved line that is joining tangentially to two given points under given direction angles. Their determination was through a series of tangents of the curve at densely lying points along the axis of the beam, using numerical methods. The function of the curve could also be given analytically, but its shape can better be controlled by numerical determination.

## 5.3 Shear force fraction transmitted by the concrete compression zone along the central part of the beam

In case of higher  $l/d$  slenderness ratios consideration of the vertical component of the internal compression force acting along the compression line – as part of the shear capacity – becomes insignificant for even very low values of  $\theta$  along the internal fraction of the beam. On the other hand it is reasonable to take into consideration a limited fraction of the great compression force acting in the concrete compression chord along this section of the beam axis, as a contribution of the compressed concrete to the shear capacity, although this is not contained by the EC2.

The earlier Hungarian reinforced concrete standard MSz 15022-71 (1971) prescribed in this respect 10% of the compression chord force as part of the shear capacity. The failure condition of the compressed-sheared concrete, based on test experiences (Szalai (1988))[9] is given by the expression below:

$$\tau_{ck} = f_{ck} \left( \frac{f_{ct,k}}{f_{ck}} + \frac{\sigma_c}{f_{ck}} \right) \left( 1 - \frac{\sigma_c}{f_{ck}} \right), \quad (7)$$

where  $f_{ck}$  and  $f_{ct,k}$  are the characteristic values of the concrete uniaxial compression and tensile strengths respectively,  $\sigma_c$  is the compression stress in the compressed-sheared concrete at failure,  $\tau_{ck}$  is the characteristic value of the shear strength of the compressed-sheared concrete.

When considering shear strength  $\tau_{ck}$  equal to 10% of the compression strength  $f_{ck}$ , the compression strength will be – according to (7) – decreasing by the same extent. Numerical investigations proved that exploiting the shear strength of compressed concrete to this extent along the central part of a beam loaded by a uniformly distributed load, is sufficient for the beam to be safe against shear with minimum stirrups. The 10% reduction of the flexural-compression strength of the concrete at approximately one quarter of the span will have a relatively small influence on the necessary cross-sectional dimensions and quantity of the tension reinforcement, when compared with the positive effect that limited shear strength exploitation will have on the quantity of shear reinforcement. Parametric investigation of this problem will naturally be needed.

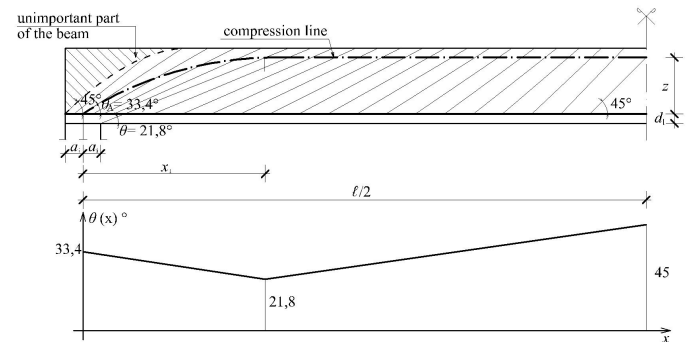


Fig. 5. The variation of the strut inclination angle  $\theta(x)$  and visualization of the variation along the left half of a beam for  $\theta=21,8^\circ$

Our model proposal can then be completed: the vaulted lattice model will be combined by  $0.1f_{ck}$  shear strength exploitation of the concrete compression chord along the central part of the beam.

Along the arched section of the compression line, where the vertical component of the concrete compression force results in higher contribution to the equilibration of shear than the above exploitation rate of shear strength, there is no need and is not even reasonable to take this effect into consideration. The constant direction changes of the concrete principal stresses along this section of the beam are namely taking place because the concrete supports significant shear, and this is the reason for the reduction of the concrete compression strength by the effectiveness factor  $\nu = 0.6 \cdot (1 - f_{ck}/250)$  when determining  $V_{Rd,max}$ . Accordingly, there is no need to reduce the value of  $V_{Rd,max}$  as given in EC2 by a further reduction factor. The previous two ways of considering the concrete compression force due to flexure in the top chord of the beam by determining the shear capacity can pass over to each other by respecting the greater one from among the two values: shear fraction of horizontal compression

and vertical component of diagonal compression:

$$V_{Rd,\gamma+sh} = \max(N_{cV}; 0, 1N_{cH}) \quad (8)$$

Here, in the index ( $\gamma+sh$ )  $\gamma$  relates to the inclination angle of the compression line and  $sh$  to shear strength of the compressed concrete.

#### 5.4 The rupture polygon of the vaulted lattice model

Sides of the rupture polygon are perpendicular to the compression line and parallel to the direction  $\theta(x)$  (see Fig. 6). The

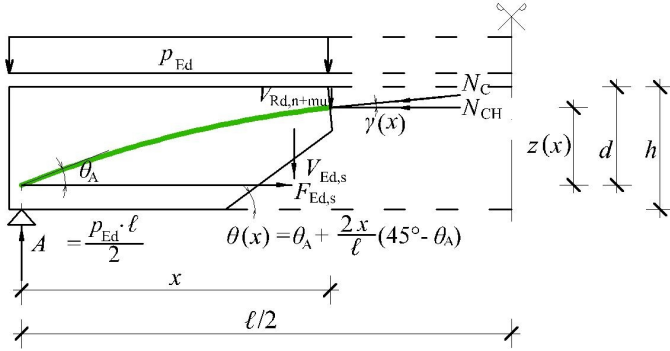


Fig. 6. Rupture polygon of the arched lattice model

concrete compression force components  $N_{cH}$  and  $N_{cV}$  can be determined from the moment equilibrium condition with respect to the point of intersection of the line of action of forces  $F_{Ed,s}$  and  $V_{Ed,s}$  by using the internal lever arm  $z(x)$  and inclination angle  $\gamma(x)$ :

$$N_{cH}(x) = \frac{A(x - 0, 5z(x) \cot \theta(x)) - p_{Ed}x(0, 5x - 0, 5z(x) \cot \theta(x))}{z(x) - 0, 5 \tan \gamma(x)z(x) \cot \theta(x)} \quad (9)$$

$N_{cV}(x)$  can then be determined by Eq. (1). The shear force fraction  $V_{Ed,s}$  to be equilibrated by the stirrups can be determined from the equilibrium of vertical forces:

$$V_{Ed,s}^{\text{arched}}(x) = A - p_{Ed}x - V_{Rd,\gamma+sh}(x) \quad (10)$$

#### 5.5 Checking of the beam end by application of the vaulted lattice model

The embedment length of the longitudinal reinforcement is determined by supposing  $45^\circ$  as approximation of the primary crack angle at the internal support face:

$$l_s = 2a_i + \sqrt{2}(h - d) - c_{\text{nom}} \quad (11)$$

The pull-out force of the tension reinforcement can be determined from equilibrium of horizontal forces:

$$F_{Ed,s} = N_{cH}(x_1) \quad (12)$$

Here,  $x_1$  is the  $x$ -coordinate of the compression line point, from which the internal edge of the support can be seen under an angle

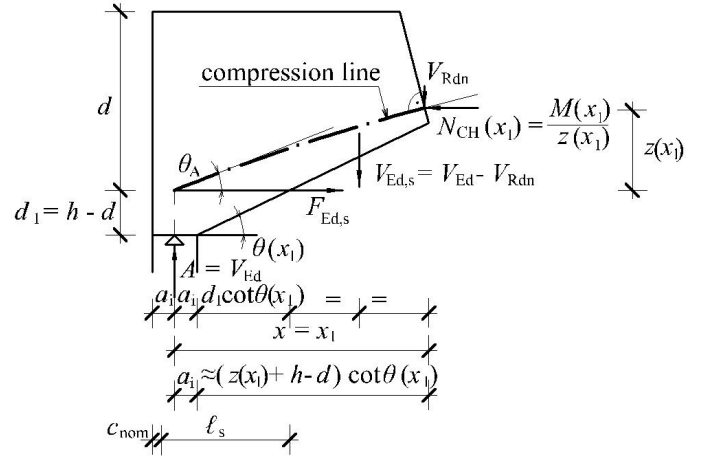


Fig. 7. Anchorage check at the beam end

$\theta = \theta_{EC2}$ :

$$x_1 \cong a_i + (z(x_1) + h - d) \cot \theta(x_1) \quad (13.a)$$

Here:

$$\theta(x_1) = \theta_{EC2} = \theta \quad (13.b)$$

Corresponding to the proposal, a tension force  $F_{Ed,s}$  should be anchored by the longitudinal reinforcement along the length  $l_s$ , which can be determined from the moment equilibrium condition concerning the rupture polygon. The point of investigation – the point along the compression line with  $x = x_1$  – can be determined by step-by-step calculation, using the numerically determined value of the  $z(x)$  compression line ordinate. Our numerical investigation resulted in the approximate value of the steel pull-out force  $F_{Ed,s}$ , as indicated below:

$$F_{Ed,s} \approx 1,1 \frac{p_{Ed}l}{2} \cot \theta_A, \quad (14)$$

that is at about 10% greater than the horizontal component of the inclined concrete compression force intersecting the axis of the tension reinforcement under the angle  $\theta_A$  above the support point. It is anyhow a more safe value than  $\Delta F_{td}$  given in EC2 (2005, (6.18)) as the additional tensile force developing in the longitudinal reinforcement due to shear:

$$F_{Ed,s}^{EC2} = \Delta F_{td} = \frac{V_{Ed,red}}{2} \cot \theta \quad (15)$$

Here,  $V_{Ed,red}$  is the shear force at distance  $d$  from the internal face of the support.  $\Delta F_{td}$  was namely determined by considering moment equilibrium condition of the parallel chord truss with effective depth  $z \approx 0.9d$ . At the end of the beam this effective depth is questionable and because the force  $F_{Ed,s}$  is proportional with  $1/z$ , the force determined by (15) seems to be underestimated. In the numerical examples the force  $F_{Ed,s}$  was determined by (14).

## 5.6 Transformation of numerical results obtained by use of the vaulted lattice model for practical applications

As the capacity of the shear reinforcement is in linear relationship with both the internal lever arm  $z$  and the cotangent of the compression strut inclination angle  $\theta$ , and according to our model proposal both of these parameters are variable along the beam axis, the fraction of the shear force that is to be equilibrated by the shear reinforcement according to (10) should be transformed in order to be comparable to the actual shear force of EC2 or to its greatest value  $V_{Ed,red}$  respectively:

$$V_{Ed,s,tr}^{arched}(x) = V_{Ed,s}^{arched}(x) \frac{z_{EC2} \cot \theta_{EC2}}{z(x) \cot \theta(x)}, \quad (16)$$

where the parameters in the denominator are those of the vaulted model and both rate-multipliers are greater than 1. Values of  $V_{Ed,s,tr}^{arched}(x)$  can then be treated as actual shear forces for design of the shear reinforcement according to EC2.

As the actual shear force is from  $V_{Ed,red}$  in direction of the centre of the span monotone decreasing, the relationship

$$\alpha_{cn} = \frac{V_{Ed,red} - \max(V_{Ed,s,tr}^{arched}(x))}{V_{Ed,red}} \quad (17)$$

can be considered as a safe quota of  $V_{Ed,red}$  which is transmitted to the supports by the arch effect and through the shear resistance of the compressed concrete of the reinforced concrete beam. By taking into consideration the favourable effect of the vaulted lattice model with compressed-sheared top chord the shear reinforcement can be designed for the force

$$V_{Ed,s,EC2}^{arched} = V_{Ed,red} - V_{Rd,cn} \quad (18)$$

where

$$V_{Rd,cn} = \alpha_{cn} V_{Ed,red} \quad (19)$$

Otherwise the design procedure of the EC2 can be followed in all respects with one only exception. The exception concerns the value of the pull-out force to be anchored by the tension reinforcement at the beam end, which is to be determined by (14). Proposal for the value of  $\alpha_{cn}$  will be given after evaluation of the numerical examples. In Fig. 8 shear force diagrams  $V_{Ed}$ ,  $V_{Ed,EC2}$ ,  $V_{Ed,s}^{arched}$ ,  $V_{Ed,s,tr}^{arched}$  and  $V_{Ed,EC2}^{arched}$  are shown for one of the numerical examples.

Shear force diagrams  $V_{Ed}$ : design value of the actual shear force,  $V_{Ed,max}$ : design value of the actual shear force at support A,  $V_{Ed,EC2}$  (or  $V_{Ed,red}$ ): design value of the actual shear force according to Eurocode 2,  $V_{Ed,s}^{arched}$ : design value of the actual shear force to be equilibrated by the shear reinforcement according to the vaulted lattice model with compressed-sheared top chord,  $V_{Ed,s,tr}^{arched}$ : transposed design value of the actual shear force to be equilibrated by the shear reinforcement according to the vaulted lattice model with compressed-sheared top chord, and  $V_{Ed,s,EC2}^{arched}$ : proposed design value of the actual shear force to be equilibrated by the shear reinforcement according to Eurocode 2, determined by taking into consideration the vaulted lattice model with compressed-sheared top chord.

## 6 Numerical examples

### 6.1 Characteristics of the investigated beams

The results of two series of numerical examples will be shown below. Emphasis will be laid on the designed shear reinforcement, the shear capacity fraction attributed to the concrete, the way of anchorage of the internal horizontal force at the support and value of the quota  $\alpha_{cn}$ . Calculations were made according to the vaulted lattice model and prescriptions of EC2.

In one of the two series of examples monolithic beams, in the other prefabricated beams were analyzed respectively, both simple supported, with data corresponding to the needs of the construction practice. The two series of beams differ mainly in geometry:

- *support length* of monolithic beams was 250 mm, that of prefabricated beams 150 mm
- *l/d slenderness ratio* of monolithic beams ranged from 14 to 18, that of prefabricated beams from 18 to 22.

Intensity of the uniformly distributed load was adopted so that the support reaction force was for all examples equal to  $0.8V_{Rd,max}$ .

For the value of the compression strut inclination angle  $\theta$  as defined by EC2,  $45^\circ$ ,  $37.5^\circ$ ,  $30^\circ$  and  $21.6^\circ$  were adopted. The value of  $\theta_A$  was then determined according to (4).

*Characteristics of monolithic beams:* concrete C30/37, reinforcement B60.50, vertical links  $\emptyset 8$ , straight longitudinal reinforcement  $\emptyset 16$ , 30 cm web thickness, 20 mm minimum concrete cover, 25 cm support length. The internal level arm  $z$  was a variable parameter between 200 and 500 mm in steps of 75 mm. The effective depth was determined by the approximation  $z = 0.9d$ . To each value of  $z$  one theoretical span was ordered so that members of the series of beams would uniformly be distributed along the slenderness domain  $14 \leq l/d \leq 18$ , characteristic for monolithic reinforced concrete beams ( $l_{eff} = 4.0, 5.0, 6.0, 7.0$  and  $8.0$  m).

*Characteristics of prefabricated reinforced concrete beams:* concrete C40/50, reinforcement B60.50, vertical links  $\emptyset 8$ , straight longitudinal reinforcement  $\emptyset 16$ , 16 cm web thickness, 20 mm minimum concrete cover, 15 cm support length. The internal level arm  $z$  was variable parameter between 300 and 700 mm in steps of 100 mm. The effective depth was determined by the approximation  $z = 0.9d$ . To each value of  $z$  one theoretical span was ordered so that members of the series of beams would uniformly be distributed along the slenderness domain  $18 \leq l/d \leq 22$ , characteristic for prefabricated reinforced concrete beams ( $l_{eff} = 7.2, 9.0, 10.5, 12.0$  and  $14.4$  m).

### 6.2 Results and evaluation

#### Results

The most important results of the numerical examples were arranged in  $2 \times 3$  tables, which are available on the home page [szi.bme.hu](http://szi.bme.hu) under munkatársak/oktatók és doktoranduszok/Draskóczy/. One table was made for  $\theta = 21.8^\circ, 30^\circ$  and  $45^\circ$

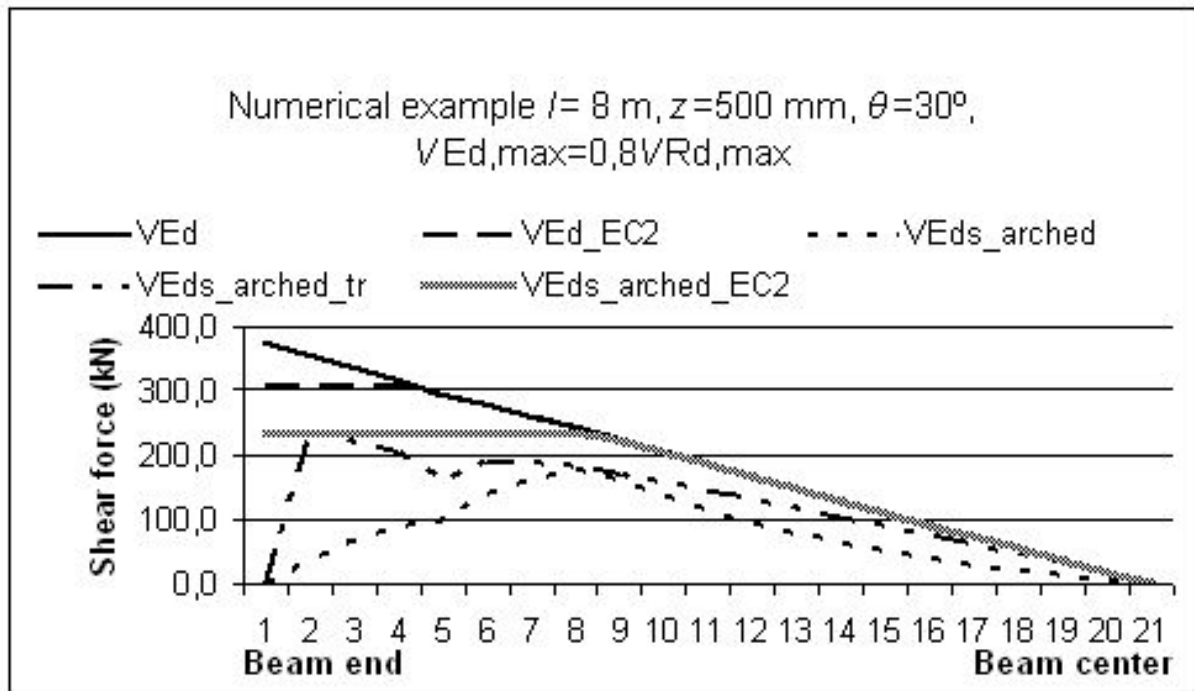


Fig. 8. Diagrams of shear forces to be equilibrated by the shear reinforcement of one of the numerical examples

compression strut inclination angles and for each angle one for monolithic, one for prefabricated beams.

On each of the tables 5 numerical examples are presented corresponding to the variable slenderness ratio  $l/d$ . After the common and individual data, stirrup spacing for the left half beam is given in three columns:

- 1 For the vaulted lattice model with compressed-sheared top chord
- 2 For the  $\theta$  strut inclination angle according to the Schlaich-Reineck strut and tie model and EC2 analysis
- 3 For our  $\theta_A - \theta$  strut inclination angle relationship proposal (4) and EC2 analysis.

Then, the shear force fractions attributed to the concrete are given, the number of links according to (1), saving of links in case of the arched model, expressed in %, when compared with results of (2) and (3) respectively. The rate  $F_{Ed,s}/F_{Rd,s}$  in the last but one row gives the fraction of the bottom reinforcement designed for moment, which is to be lead up to and anchored at the end of the beam, to equilibrate the horizontal component of the inclined concrete compression force. The force to be anchored back was determined according to (14). Then two numbers give the surplus of the shear force fraction supported by the concrete according to the vaulted model, when compared with the two kinds of EC2 analysis.

Finally, in the last line, the safe value of the quota  $\alpha_{cn}$  was given according to (17) for each of the numerical examples.

The given stirrup spacings are multiples of 25 mm and satisfy with only one exception the construction rules given in EC2: in case the spacing resulted in 25 mm – for better overview of the results – the diameter of the stirrups was not increased.

### Results evaluation

In Table 2 intervals of the quota  $\alpha_c$  are given as obtained in a series of the numerical examples. Values for  $\theta = 21.8^\circ$  are definitely smaller. This is the consequence of the increase of the rate factor  $z_{EC2}/z(x)$ , due to the little lever arm  $z(x)$  near the support in case of the vaulted model. For greater values of  $\theta$  the minimum value of  $\alpha_c$  will be obtained – as mentioned earlier – at approximately the quarter point of the span, and will only be little under 0.25. It is a numerical proof for that *compression strut inclination angles  $\theta$  smaller than  $30^\circ$  have little advantage, because beside anchorage problems of the bottom bars, the arching effect can scarcely be exploited.*

Tab. 2. Intervals of the quota  $\alpha_{cn}$  for the investigated series of numerical examples

$\theta (\theta_A)$	Prefabricated beams	Monolithic beams
$21.8^\circ (33.4^\circ)$	0.210-0.184	0.220-0.160
$30^\circ (37.5^\circ)$	0.305-0.297	0.402-0.345
$37.5^\circ (41.25^\circ)$	0.325-0.280	0.325-0.267
$45^\circ (45^\circ)$	0.303-0.275	0.269-0.231

Based on results of the numerical investigation above the following modifications are proposed for the design of shear reinforcement (vertical stirrups) of reinforced concrete beams, loaded predominantly by uniformly distributed load:

The condition  $V_{Ed,max} \leq V_{Rd,max}$  should always be fulfilled. If  $V_{Ed,red} > V_{Rd,c}$ , the shear reinforcement (vertical stirrups) must be designed. In this case:

$$V_{Rd} = V_{Rd,cn} + V_{Rd,s} \geq V_{Ed}, \quad (20)$$

where (19):  $V_{Rd,cn} = \alpha_{cn} V_{Ed,red}$

**Tab. 3.** Comparison of the results of EC2 calculations, tests and arched model calculations

Beam code	original EC2 calculation				reason of failure in the test	EC2 calculation taking into consideration results of the vaulted lattice model			
	$P_{Rdmax}$ (kN/m)	$\theta_{pRdmax}$ (°)	reason of reaching $P_{Rdmax}$	$p_u/p_{Rdmax}$		$P_{Rdmax}$ (kN/m)	$\theta_{pRdmax}$ (°)	reason of reaching $P_{Rdmax}$	$p_u/p_{Rdmax}$
AN1K1	184.0	33	$M_{Rd}$	1.73	$M_{Ru}$	184.0	33	$M_{Rd}$	1.73
AN1K2	163.3	33	$V_{Rdmax}$	1.83	$M_{Ru}$	174.9	39	$V_{Rdmax}$	1.70
AN1K3	131.1	24	$V_{Rds}$	2.01	$F_{Rsu}$	144.6	27	$V_{Rdmax}$	1.82
AN1K4	98.3	21.6	$V_{Rds}$	2.73	$F_{Rsu}$	128.3	21.6	$V_{Rdmax}$	2.09
AN2K1	186.2	30	$M_{Rd}$	1.54	$M_{Ru}$	186.2	33	$M_{Rd}$	1.54
AN2K2	186.3	30	$M_{Rd}$	1.66	$M_{Ru}$	186.2	36	$M_{Rd}$	1.66
AN2K3	147.4	21.6	$V_{Rds}$	1.67	$F_{Rsu}$	161.8	24	$F_{Rds}$	1.52
AN2K4	98.3	21.6	$V_{Rds}$	2.17	$F_{Rsu}$	130.7	21.6	$V_{Rds}$	1.63
AN3K1	181.9	39	$M_{Rd}$	1.65	$M_{Ru}$	181.9	39	$M_{Rd}$	1.65
AN3K2	171.2	33	$V_{Rdmax}$	1.42	$F_{Rsu}$	181.4	39	$M_{Rd}$	1.34
AN3K3	147.4	21.6	$V_{Rds}$	1.72	$F_{Rsu}$	161.8	24	$F_{Rds}$	1.57
AN3K4	98.3	21.6	$V_{Rds}$	1.97	$F_{Rsu}$	130.3	21.6	$V_{Rdmax}$	1.49

Here

$$\alpha_{cn} = 0.25 \quad \text{if} \quad 30^\circ \leq \theta \leq 45^\circ \quad (21)$$

The pull-out force  $F_{Ed,s}$  at the beam end should be determined by (14), the compression strut inclination angle  $\theta_A$  at the support point by (4).

Values of  $V_{Rd,c}$ ,  $V_{Rd,max}$  and  $V_{Rd,s}$  will all be determined according to EC2.

### 7 Evaluation of test results by application of the vaulted model

#### Conclusions

- For each of the three groups of beams it can be observed that with increasing spacing of stirrups (see Fig. 1) the maximum load-bearing capacity will be reached generally by decreasing strut inclination angles, and that through the vaulted model the strut inclination angle  $\theta$  at failure is somewhat higher. From these tendencies the following conclusions can be drawn: a) by decreasing shear reinforcement intensity beams tend to resist by reaching smaller strut inclination angles; b) in case of the vaulted model higher resistance load intensity at greater strut inclination angle can be determined.
- For beam type A the calculation according to EC2 results in failure of stirrups for every second beam, whereas by application of the vaulted model only for one of the 12 beams which is in better accordance with the real failure modes at tests.
- The rate  $p_u/p_{Rd}$  is by application of the vaulted model – for beam type A – smaller or at most equal to the rate determined according to EC2 calculations, and is nearer to the desirable value of approximately 1.5.

### 8 Summary of conclusions

Based on beam tests results and results of numerical examples obtained by applying a vaulted D-region lattice model proposal,

the author proposes the use of about 30° compression strut inclination angles at extreme supports of reinforced concrete beams, loaded predominantly by uniformly distributed load, which results in about 25% less transverse reinforcement intensity and – because of end anchorage problems – some increase of the longitudinal bottom reinforcement at the beam end. This kind of change fits well to present technological demands. Further test investigation is needed to elaborate constructional rules for design practice.

### References

- Draskóczy A.** *Main Directions of Standardization in Shear Design*, Concrete Structures, Annual Technical Journal of the Hungarian Group of FIB **4** (2003), 59-66.
- EUROCODE 2: Design of Concrete Structures**, General Rules and Rules for Buildings, December 2003. Final draft prEN 1992-1-1.
- Rojek R, Bürklin A, Romer R, Keller T.** *Stahlbetonanalyse 21, Teil 1: Tragverhalten ohne Stegbewehrung*, Forschungsbericht des Kompetenzzentrums Konstruktiver Ingenieurbau der Fachhochschule Augsburg, 2003.
- Reineck K H.** *Ein mechanisches Modell für das Tragverhalten von Stahlbetonbauteilen ohne Stegbewehrung*, Bauingenieur **66** (1991), 323-332.
- Kollár L P, Dulácska E.** *Az ívhatás figyelembe vételének módja vasbeton gerendákban az Eurocode szerint*, Vasbetonépítés **10** (2009). (under edition in Hungarian).
- Hegger J, Görtz S.** *Querkraftmodell für Bauteile aus Normalbeton und Hochleistungsbeton*, Beton- und Stahlbetonbau **101** (2006), no. 9, 695-705, DOI 10.1002/best.200600498.
- MSZ 15022/1-71:Épületek teherhordó szerkezetének tervezése, Vasbeton szerkezetek**, 1971.
- Schlaich J, Schäfer K.** *Konstruieren im Stahlbetonbau, Beton-Kalender Teil II*, Berlin-München: Ernst und Sohn, 1998.
- Szalai K.** *Vasbeton szerkezetek, Vasbeton szerkezetek szilárdságtana*, Budapest, 1988. Text-book.